ELSEVIER

Journal of Non-Crystalline Solids 222 (1997) 137–143

JOURNAL OF
NON-CRYSTALLINE SOLIDS

Role of network connectivity on the elastic, plastic and thermal behavior of covalent glasses

Xingwei Feng, W.J. Bresser, Min Zhang[1], B. Goodman[2], P. Boolchand*

Department of Electrical and Computer Engineering and Computer Science, University of Cincinnati, Cincinnati, OH 45221-0030, USA

Abstract

Experiments on chalcogenide glasses show that local elasticity as measured by Raman scattering and the kinetic heat-flow near T_g as established from temperature modulated differential scanning calorimetry each display a threshold behavior associated with network connectivity as defined by the mean coordination, $\langle r \rangle$, near $\langle r \rangle = \langle r \rangle_c \simeq 2.40$. Network plasticity of amorphous group IV networks as deduced from nanometer-indentation hardness measurements varies linearly with $\langle r \rangle$ once $\langle r \rangle > 2.40$. Consequences of these results connecting physical behavior of covalent networks with their connectivity are discussed. © 1997 Elsevier Science B.V.

1. Introduction

One of the success stories in glass science is the correlation in covalently bonded networks between a variety of physical properties and network connectivity as defined by the mean coordination number $\langle r \rangle$. In Table 1 we summarize experimental results and numerical simulations that bear on this correlation [1–19]. These observations underscore the central role of nearest-neighbor valence force fields as effective constraints [20] in determining the physical behavior of covalent network glasses. In this work we shall discuss some recent results from several techniques, namely, Raman scattering, temperature modulated differential scanning calorimetry, and nanometer-indentation hardness measurements that show the above mentioned correlation in a rather striking fashion and provide additional insights.

2. Constraint theory, random network simulations, local elasticity and Raman scattering

2.1. Constraint theory and random network simulations

A covalently bonded random network progressively stiffens as its connectivity or mean coordination number, $\langle r \rangle$, increases. Networks consist-

---

[1] Present address: Actel Corporation, Sunnyvale, CA 94086-4533, USA.

[2] Present address: Department of Physics, University of Cincinnati, Cincinnati, OH 45221-0011, USA.

* Corresponding author. Tel.: +1-513 556 4758; fax: +1-513 556 7326; e-mail: pboolcha@ececs.uc.edu

PII S0022-3093(97)00357-8

Table 1
Correlation of physical properties of glasses with network connectivity in network glasses

Observable	Glass system	Results	Authors (year)
Molar volumes	Ge_xSe_{1-x}	A broad minimum near $x \sim 0.23$, $\langle r \rangle = 2.46$	Feltz et al. (1983) [1]
^{129}I Mössbauer site occupancy	Ge_xSe_{1-x}	A local max. near $x \sim 0.23$, $\langle r \rangle = 2.46$	Bresser et al. (1986) [2]
Raman $Ge(Se_{1/2})_4$ A_1 mode frequency	Ge_xSe_{1-x}	$\nu_1(x)$ shows kink near $x \sim 0.2$, $\langle r \rangle = 2.40$	Murase et al. (1986) [3]
Mössbauer quadrupole splitting, Raman modes, glass structure	Si_xTe_{1-x}	Qualitative change in structure at $x = 0.2$, $\langle r \rangle = 2.40$	Norban et al. (1986) [4]
Insulator → metal transition pressure P_T	Ge–Se, Si–Te	P_T shows a sharp kink at $\langle r \rangle = 2.4$, $\langle r \rangle = 2.40$	Asokan et al. (1988) [5]
Ultrasonic bulk moduli (C_{11}, C_{44})	Ge_xSe_{1-x}	Linear variation with x, no anomaly observed near $x \sim 0.20$	Yun et al. (1989) [6]
^{119}Sn Lamb–Mössbauer factor $f(0)$	$(Ge_{0.99}Sn_{0.01})_xSe_{1-x}$	A kink observed in $f(0)$ at $x \sim 0.20$	Boolchand et al. (1990) [7]
ΔCp, $E_a{}^{\eta}$ and $E_a{}^{H}$	As–Ge–Se	Minimum in observables near $\langle r \rangle = 2.4$	Tatsumisago et al. (1990) [8]
Inelastic neutron scattering	As–Ge–Se	Obsv. floppy modes at 5 meV	Kamitahara et al. (1991) [9]
^{125}Te Lamb–Mössbauer factors	$(Na_2O)_x\ (TeO_2)_{1-x}$	Kink in $f(0)$ near $x \sim 0.18$	Zhang and Boolchand (1994) [10]
Thermal expansion $\Delta\alpha$, heat capacity ΔC_p	Ge–Se and Ge–Sb–Se	$\Delta\alpha$, ΔC_p both show a min. at $\langle r \rangle = 2.4$	Senapati and Varshnaye (1995) [11]
Non-radiative decay rate of H_2O guest molecule	Ge–As–Se	A kink obsv. near $\langle r \rangle = 2.4$	Uebbing and Sievers (1996) [12];
Raman A_1 mode freq. shift	Ge_xSe_{1-x} and Ge_xS_{1-x}	$\nu_1(x)$ in both systems show a discontinuity at $x \sim 0.225$, $\langle L \rangle = 2.46(1)$	Phillips (1996) [13] Feng et al. (1996) [14]
E_a (stress relaxation)	Ge–As–Se	Obsv. a min near $\langle r \rangle = 2.4$	Bohmer and Angell (1992) [15]
Numerical experiments:			
Floppy modes and elastic constants	Bond depleted diamond network	Linear at $\langle r \rangle < \langle r \rangle_c$; exponential at $\langle r \rangle > \langle r \rangle_c$	Franzblau and Tersoff (1992) [16];
C_{11} and C_{44}		$C_{11} \sim (\langle r \rangle - \langle r \rangle_c)^{1.4}$	He and Thorpe (1983) [18]
Floppy modes	2D triangular central force networks	Bond conc. $p = 0.6603(3)$ at stiffness threshold	Jacobs and Thorpe (1995) [19]

ing of chains (every atom having two nearest neighbors, $r = 2$), as in elemental S or Se, are mechanically floppy because the number of nearest neighbors bonding constraints per atom ($= 2$) are less than 3, the degrees of freedom per atom. The reverse is the case for networks composed of tetrahedral units ($r = 4$), such as those of elemental Si or Ge, which are thus intrinsically rigid.The mean-field theory [20,21] of constraints due to bond-stretching and bond-bending forces, on atomic displacements in random networks, counts the excess or deficit of constraints per atom, n_c (relative to $n_c = 3$), in terms of $\langle r \rangle$. The critical value of $\langle r \rangle$ is found to be $\langle r \rangle_c = 2.40$ (corresponding to $n_c = 3$), below which there are $5/2(\langle r \rangle_c - \langle r \rangle)$ floppy modes per atom. Thus at a critical mean coordination, $\langle r \rangle_c = 2.40$, the number of constraints per atom (n_c) equals the degrees of freedom per atom (n_d), and mean-field theory predicts the onset of rigidity [20,21].

Numerical 'experiments' have been performed [16–19] on models of network glasses constructed from bond-depleted diamond lattice to examine the vibrational behavior as a function of network connectivity $\langle r \rangle$. In these computer simulations a Keating potential is used which takes into account bond stretching and bond bending forces between nearest-neighbor atoms. In the macroscopically rigid region ($\langle r \rangle > \langle r \rangle_c$), these simulations show that elastic constants C display a power-law behavior with $\langle r \rangle$, i.e. $C \sim (\langle r \rangle - 2.4)^p$ with $p = 1.40$. To date there is no theoretical basis for this number for the exponent.

2.2. Local elasticity and Raman scattering

In binary Ge_xX_{1-x} glasses where X = S, Se or Te, tetrahedral $Ge(X_{1/2})_4$ units constitute one of the principal building blocks of the network backbone. Corner-sharing (CS) $Ge(X_{1/2})_4$ units have a Raman active A_1 mode which is a symmetric breathing motion of the four chalcogens (X) about the central Ge atom. The scale for the underlying mode frequency, $\nu = \sqrt{\alpha_{\text{eff}}/m_x}$, is set largely by the Ge–X bond-stretching force constant, α, and the reduced mass of the chalcogen, m_x. The bridging angle about the chalcogen atom between CS tetrahedra deviates from $\pi/2$ by typically about 10°, so that the radial displacements of the A_1 modes of X bridged tetrahedra are coupled in energy. This inter-tetrahedral coupling gives rise to mode frequency changes. The smallness of the frequency shifts in glasses with composition suggests that each A_1 mode is weakly coupled to a few tetrahedra. Furthermore, since CS tetrahedra represent the majority component of the Ge_xX_{1-x} glassy networks when $x \sim 0.2$, the squared frequency $\nu^2 = \alpha_{\text{eff}}/m_x$ becomes a direct probe of intermediate-range network elasticity.

We have performed [14] micro-Raman measurements on binary Ge-Se (Ge-S) glasses using < 1 mW of 647.1 nm (514.5 nm) exciting radiation. The A_1 symmetric stretch modes of corner-sharing (CS) $Ge(X_{1/2})_4$ units occur at about 200 cm^{-1} for X = Se, and at 340 cm^{-1} for X = S glasses. The composition dependence of the mean frequency, $\nu(x)$, of the A_1 mode for X = Se, obtained by least-squares fitting the observed lineshapes, is reproduced in Fig. 1a. We find that $\nu(x)$ increases linearly in the $0.10 < x < 0.22$ composition range, displays a discontinuous change [14] between $x = 0.225$ and $x = 0.230$, and then increases superlinearly at larger x. To describe the super-linear variation, we have fit ν^2 using the following power-law [16–19]:

$$\nu^2 - \nu_c^2 = A(\langle r \rangle - \langle r \rangle_c)^p. \tag{1}$$

In Eq. (1), the mean coordination of the binary glasses is $\langle r \rangle = 2(1 + x)$, since Ge and the chalcogen atoms X are, respectively, four- and twofold coordination, ν_c is the Raman shift corresponding to $x_c = 0.23$ or $\langle r \rangle_c = 2.46$. The power, p, obtained by plotting log $(\nu^2 - \nu_c^2)$ against log $(\langle r \rangle - \langle r \rangle_c)$ (see Fig. 2), is $p = 1.29(3)$ and $p = 1.33(1)$ for the S- and Se-glasses, respectively, at 78 K. At 300 K, somewhat lower values $p = 1.21(2)$ and $p = 1.20(3)$, respectively, are obtained. The numbers in parentheses are the magnitude of the uncertainties in the last digit.

We interpret the discontinuity in Raman mode frequency shifts near $\langle r \rangle_c = 2.46(1)$ as evidence [14] of a stiffness threshold in these glasses. It is remarkable how close the lower temperature (T

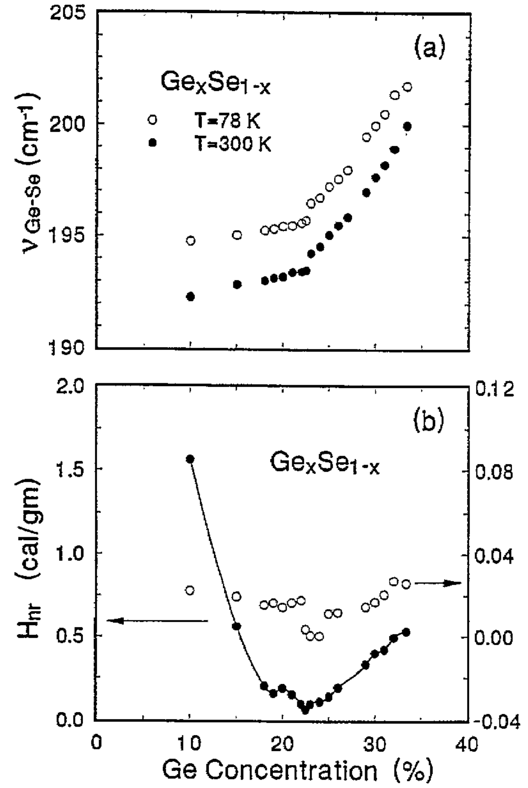

Fig. 1. (a) Raman A_1 mode frequency shift ν of $Ge(Se_{1/2})_4$ units. (b) Non-reversing heat flow ΔH_{nr} at T_g, in Ge_xSe_{1-x} glasses studied as a function of x showing a threshold behavior near $x = 0.23$ corresponding to stiffness transition. See [14] for additional details. The line in (b) is drawn as a guide for the eye.

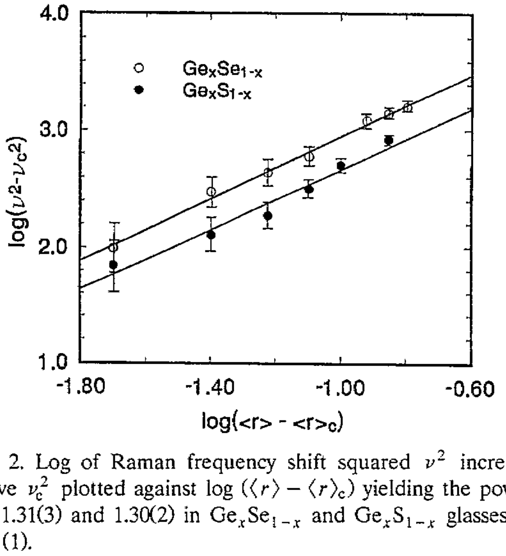

Fig. 2. Log of Raman frequency shift squared ν^2 increase above ν_c^2 plotted against log ($\langle r\rangle - \langle r\rangle_c$) yielding the power $p = 1.31(3)$ and 1.30(2) in Ge_xSe_{1-x} and Ge_xS_{1-x} glasses of Eq. (1).

$= 78$ K) of p in Eq. (1) is to the power, p, in Section 2.1 for the numerically found concentration dependence of the elastic constants at $T = 0$. Recall that only short-range forces (Keating) are included in the former calculations. This agreement suggests a picture of local elasticity dominated by short-range forces for the intrinsically short wavelength coupled A_1 modes.

3. Structural relaxation of a glass network at T_g and temperature modulated differential scanning calorimetry

The recent introduction of temperature-modulated differential scanning calorimeters [22] (MDSC) has opened the possibility to deconvolute the reversing (ΔH_r) heat flow at T_g from the total heat flow (ΔH_t), and thus obtain the non-reversing heat flow ($\Delta H_{nr} = \Delta H_t - \Delta H_r$) component. This resolution is generally achieved by imposing a sinusoidal temperature modulation on a linear temperature ramp to extract the heat-flow component (ΔH_r) to the sample that tracks the sinusoidal T-modulation. The non-reversing heat-flow at T_g provides a measure of energy dissipated in molecular reorganization of a glass as it melts when $T \rightarrow T_g$.

We have measured ΔH_{nr} as a function of $\langle r\rangle$ for both Ge_xS_{1-x} and Ge_xSe_{1-x} glasses [14]. The results for selenide glasses appear in Fig. 1b. $\Delta H_{nr}\langle r\rangle$ displays a near-parabolic dependence on $\langle r\rangle$ with a local minimum near $\langle r\rangle = 2.46$, a composition which coincides [14] with the onset of network stiffness in the Raman scattering experiments on these glasses. The $\Delta H_{nr}(\langle r\rangle)$ variation (Fig. 1b) is reminiscent of the activation energy $\Delta E(\langle r\rangle)$ for tensile stress relaxation variation with $\langle r\rangle$ in chalcogenide glasses which also displays a local minimum near $\langle r\rangle = \langle r\rangle_c$ [15].

Structural arrest of a network upon undercooling freezes in stresses which are spatially localized at fragile segments. Specifically, the frozen-stress is localized near units such as Se_8 monomers and Se_n-chain segments, that proliferate at small x ($x < 0.20$), or edge-sharing tetrahedra that occur at large x ($x > 0.25$) in these glasses. Upon heating, these fragile units relax with large energy barriers, leading to an increase in ΔH_{nr}. Near the composition $x = 0.23$ or $\langle r\rangle =$

2.46, a combination of corner-sharing tetrahedra- and chain-fragments form the structural elements of the 'strong' glass. Apparently, at this composition, frozen stress is most uniform spatially [23], and structural relaxation of the network proceeds with a minimum of an energy barrier. These basic ideas underline the observed threshold behavior in $\Delta H_{nr}(\langle r \rangle)$ or $\Delta E(\langle r \rangle)$ when $\langle r \rangle$ approaches $\langle r \rangle_c$.

4. Constraint theory, nanometer-indentation hardness and network connectivity

4.1. Constraints and network plasticity

Hardness is an intrinsically plastic property of a material. On a macroscopic level, it is physically related to plastic flow when work-hardening of a material occurs. On a microscopic level, it is related to plastic flow, usually to movement of dislocations in a crystalline material. This phenomenon is to be contrasted to elastic deformation of a solid which is an intrinsically reversible process.

Within the constraint theory of glasses [23], interatomic forces provide a measure of local softness or stiffness of a network. For undercoordinated networks the local softness manifests itself in floppy modes which have been observed [9] in inelastic neutron-scattering and Lamb–Mössbauer factor [7] measurements. For overcoordinated networks such as diamond, silicon and SiC, the local stiffness is connected with plasticity of the materials. Constraint counting algorithms reveal that the average number of constraints/atom increases linearly with average coordination number. It is reasonable to expect nanometer-indentation hardness (NIH) to scale linearly with the number of constraints/atom or the mean coordination number for each of the tetrahedral solids. In nanometer-indentation measurements [23], we can operationally separate the elastic from the strictly plastic behavior of a viscoelastic material. Application of a load leads to a displacement of the indenter in the sample and upon removal of the load an elastic recovery of the sample will occur [24,25], thus permitting the plastic and elastic displacement to be decoupled from the total displacement. For this reason NIH measurements can provide a reliable measure of network plasticity.

4.2. NIH of hydrogenated amorphous group IV networks

Another interesting correlation of network connectivity is seen in the systematics of indentation hardness (NIH) of hydrogenated Si, SiC and C (diamond). The crystalline structures consist of ordered networks of tetrahedral building blocks and possess [24] NIH values of ~ 10 GPa, 30 GPa, and 100, and for which $n_c = 5/2\langle r \rangle - 3 = 7$ since $r = 4$, and one can define a hardness index $h = n_c = 4$, respectively. The increasing hardness measured in the Si → SiC → C (diamond) sequence is due to the increasing bond strength of sp^3 covalent bonds as nearest-neighbor distances decrease. To correlate hardness of corresponding hydrogenated alloys with h, it is reasonable to postulate [24] the form

$$\mathrm{NIH} = \alpha h, \tag{2}$$

where α is the chemical-bond scale factor and h represents the dependence of NIH on the network topology or microstructure within the constraint-counting description. Eq. (2) permits us to separate the chemical effects (α) from the morphological (h) ones contributing to NIH. Based on the measured NIH of the crystalline tetrahedral semiconductors, (i.e. at the value $h = 4$) one establishes directly the chemical bond scale factor $\alpha = 26.25$ GPa for diamond, $\alpha = 7.5$ GPa for SiC and $\alpha = 2.5$ GPa for Si. Thin-films of diamond-like carbon (DLC), silicon carbide (SC) and amorphous-silicon (α-Si) have been prepared by plasma decomposition of various hydrocarbons and silane precursors by several groups. Jiang et al. [25] and Tamor et al. [26] have prepared DLC-films using RF plasma decomposition of methane. Weiler et al. [27] used chemical vapor depositions with plasma beam sources of acetylene as a precursor to deposit DLC-films. Their films displayed a lower hydrogen content and larger NIH values than those reported by Jiang et al. Graphite-like sp^2 and diamond-like sp^3 bonding configurations are prevalent in these films with no detectable evidence of sp-like twofold coordinated structures.

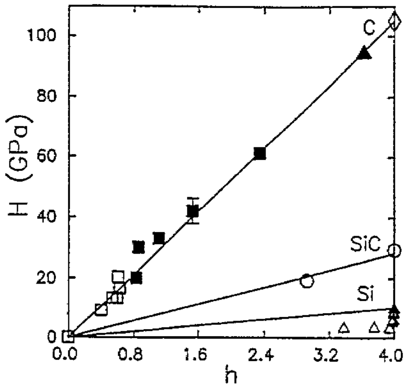

Fig. 3. Measured NIH in GPA of DLC-films, SiC-films and amorphous Si films compared to predicted hardness (continuous lines) based on mean-field constraint counting procedures. See Ref. [24] for details.

By establishing the amount of bonded hydrogen in these films, and the ratio of sp^2 to sp^3 configuration, one can calculate the hardness index h of the films from the measured hydrogen content. As has been shown elsewhere [28], it is meaningful to include the one-fold coordinated atoms in the constraint counting because they affect the number of constraints per atom. In Fig. 3, we plot the measured NIH in GPa (H) as a function of h. The NIH results on DLC-films scale linearly with h rather well. The correlation shown in Fig. 3 is suggestive that in these films hydrogen is bonded to sp^2- and sp^3-carbon but not to sp-carbon.

5. Conclusions

The role of network connectivity (as defined by mean-coordination $\langle r \rangle$) on the elastic-, plastic- and thermally-induced structural relaxation of covalently bonded networks is analyzed from results of recent Raman scattering, indentation hardness and non-reversing heat-flow measurements at T_g in MDSC measurements. Each of these physical observables displays a characteristic dependence on $\langle r \rangle$; with a resolved change near $\langle r \rangle = \langle r \rangle_c$ corresponding to the stiffness transition. The local elasticity, increases linearly with $\langle r \rangle$ at $\langle r \rangle < \langle r \rangle_c$, is discontinuous near $\langle r \rangle = \langle r \rangle_c$, and thereafter increases as a power-law, $(\langle r \rangle - \langle r \rangle_c)^p$, with $p \simeq 1.4$. The hardness is vanishing at $\langle r \rangle < \langle r \rangle_c$, and it increases nearly linearly with $\langle r \rangle$ once $\langle r \rangle > \langle r \rangle_c$. Finally, the kinetic heat-flow at T_g, which is related to thermally-induced structural relaxation of the network, displays a local minimum at $\langle r \rangle = \langle r \rangle_c$. The latter behavior is indicative of a uniform distribution of frozen-in stress [23] with small energy barriers between various states of structural relaxation when the network is optimally coordinated at the rigidity percolation threshold.

Acknowledgements

This work is supported by the National Science Foundation grants DMR-92-07166 and DMR-93-09061.

References

[1] A. Feltz, H. Aust, A. Blyer, J. Non-Cryst. Solids 55 (1983) 179.
[2] W.J. Bresser, P. Boolchand, P. Suranyi, Phys. Rev. Lett. 56 (1986) 2493.
[3] K. Murase, T. Fukunaga, Mater. Res. Soc. Symp. 61 (1986) 101.
[4] B. Norban, D. Persing, R.N. Enzweiler, P. Boolchand, J.E. Griffiths, J.C. Phillips, Phys. Rev. B 36 (1987) 8109.
[5] S. Asokan, E.S.R. Gopal, G. Parthasarathy, Phys. Rev. B 35 (1987) 8369.
[6] S.S. Yun, H. Li, R.L. Cappelletti, P. Boolchand, R.N. Enzweiler, Phys. Rev. B 39 (1989) 8702.
[7] P. Boolchand, R.N. Enzweiler, R.L. Cappelletti, W.A. Kamitakahara, Y. Cai, M.F. Thorpe, Solid State Ionics 39 (1980) 81.
[8] M. Tatsumisago, B.L. Halfpap, J.L. Green, S.M. Lindsay, C.A. Angell, Phys. Rev. Lett. 64 (1990) 1549.
[9] W.A. Kamitakahara, R.L. Cappelletti, P. Boolchand, B. Halfpap, F. Gompf, D.A. Neumann, H. Mutka, Phys. Rev. B 44 (1991) 94.
[10] M. Zhang, P. Boolchand, Science 266 (1994) 1355.
[11] U. Senapati, A.K. Varshneya, J. Non-Cryst. Solids 185 (1995) 289.
[12] B. Uebbing, A.J. Sievers, Phys. Rev. Lett. 76 (1996) 932.
[13] J.C. Phillips, Phys. Rev. B 54 (1996) R6807.
[14] X. Feng, W.J. Bresser, P. Boolchand, Phys. Rev. Lett. 78 (1997) 4422.
[15] R. Bohmer, C.A. Angell, Phys. Rev. B 45 (1992) 10091.
[16] D.S. Franzblau, J. Tersoff, Phys. Rev. Lett. 68 (1992) 2172.
[17] S.P. Obukhov, Phys. Rev. Lett. 74 (1995) 4472.

[18] H. He, M.F. Thorpe, Phys. Rev. Lett. 54 (1985) 2107.
[19] D.J. Jacobs, M.F. Thorpe, Phys. Rev. Lett. 75 (1995) 4051.
[20] J.C. Phillips, J. Non-Cryst. Solids 34 (1979) 153; Physics Today 35 (1982) 27.
[21] M.F. Thorpe, J. Non-Cryst. Solids 57 (1983) 355.
[22] B. Wunderlich, Y. Jin, A. Boller, Thermochim. Acta 238 (1994) 277.
[23] J.C. Phillips, Rep. Prog. Phys. 59 (1996) 1133.
[24] P. Boolchand, M. Zhang, B. Goodman, Phys. Rev. B 53 (1996) 11488.
[25] X. Jiang, K. Reichelt, S. Stritzker, Appl. Phys. Lett. 58 (1991) 592.
[26] M.A. Tamor, W.C. Vassell, K.R. Carduner, Appl. Phys. Lett. 58 (1991) 592.
[27] M. Weiler, R. Kleber, S. Sattel, K. Jung, H. Ehrhart, G. Jungnickel, S. Deutschmann, V. Stephen, P. Blanek, Th. Fraunheim, Diamond Related Mater. 3 (1994) 245.
[28] P. Boolchand, M.F. Thorpe, Phys. Rev. B 50 (1994) 10366.